

Mesh-free simulations of the Kelvin-Helmholtz instability in the kinetic regime

B. Steinbusch¹, P. Gibbon^{1,2}, R.D. Sydora³

¹ Institute for Advanced Simulations, Jülich Supercomputing Centre,
Forschungszentrum Jülich GmbH, D-52425 Jülich, Germany

² Centre for Mathematical Plasma Astrophysics, Department of Mathematics,
Katholieke Universiteit Leuven, Belgium

³ Department of Physics, University of Alberta,
Edmonton, Alberta T6G 2E1, Canada

Introduction

In this paper, we use a novel mesh-free model – see [1, 2, 3] – for two-dimensional electrostatic plasmas with a static magnetic field to simulate various scenarios. We start with a warm plasma having a completely homogeneous density and compare the mode content of our solution to a direct numerical solution of the analytic dispersion relation. Next, we turn to a well-studied set-up that exhibits the classical plasma Kelvin-Helmholtz (KH) instability and compare growth-rates between our model and a more traditional particle-in-cell (PIC) method. Finally, we propose a new scenario, where the boundary layer between a vacuum and a two-species plasma develops a sheared velocity field and becomes unstable with characteristics similar to the classical KH instability.

Warm magnetized plasma with a homogeneous density

First, we use our computer model to simulate a warm magnetized plasma with a homogeneous density. The plasma fills a square box of side length $L = 100r_{L,i}$ with periodic boundary conditions in the x and y directions. All system quantities are assumed to be constant in the direction of the background magnetic field $\mathbf{B}_0||\hat{\mathbf{z}}$. The box contains 10^7 particles each for two species with a mass ratio $\mu = 16$ and temperature ratio $\tau = 1$, the background magnetic field has a strength of $B_0 = 2$. We simulate the dynamics of the system for a duration $0 \leq \omega_{c,i}t \leq 60$ in discrete time steps $\omega_{c,i}\Delta t = 0.0067$.

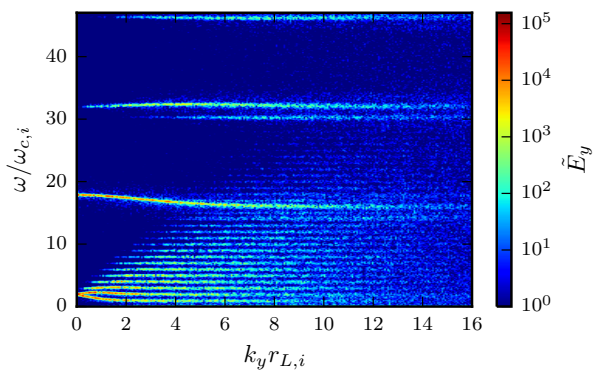


Figure 1: Frequency/wave number spectrum

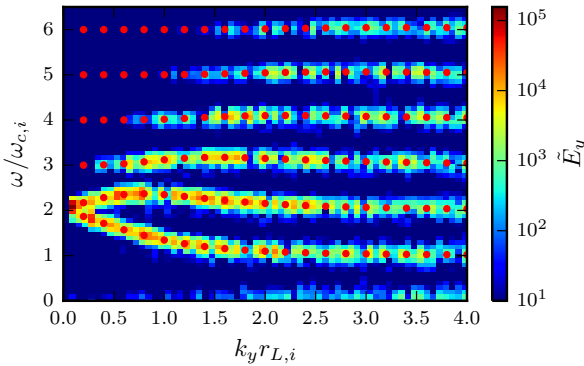


Figure 2: Zoom of figure 1, with analytic dispersion relation as red dots with the predictions and are also comparable to a study of the same set-up using a traditional PIC code.

The classical Kelvin-Helmholtz scenario in warm magnetized plasmas

Next, we use our method to reproduce experiment I from [4] and simulate the classical KH scenario with two counter-streaming half spaces. The simulation region spans an area of $L_x \times L_y = 25.6 \times 102.4 r_{L,i}^2$ with periodic boundary conditions in the y direction. We use about 10^7 particles for both species with a mass ratio of $\mu = 16$ with a slight excess of electrons concentrated in the center of the geometry to create a hyperbolic tangent electric field profile of width $a = r_{L,i}$ in the y direction driving a sheared $\mathbf{E} \times \mathbf{B}$ that feeds the instability. The magnetic field is $B_0 = 2$.

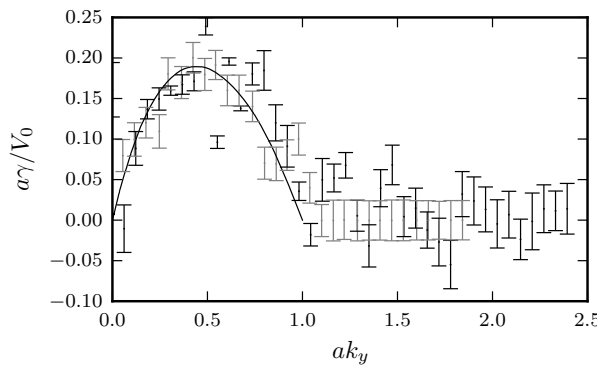


Figure 4: Comparison of growth rates

Figure 1 shows the spatial and temporal mode content of the y component of the electric field. It contains multiple ion cyclotron modes separated by $\omega_{c,i}$ and also reproduces some electron modes at multiples of $\omega_{c,e} = 16\omega_{c,i}$.

Figure 2 shows a zoom of the same data with a numeric solution of the analytic dispersion relation [5] overlaid as red dots. The modes contained in our results agree well

with the predictions and are also comparable to a study of the same set-up using a traditional PIC code.

The classical Kelvin-Helmholtz scenario in warm magnetized plasmas

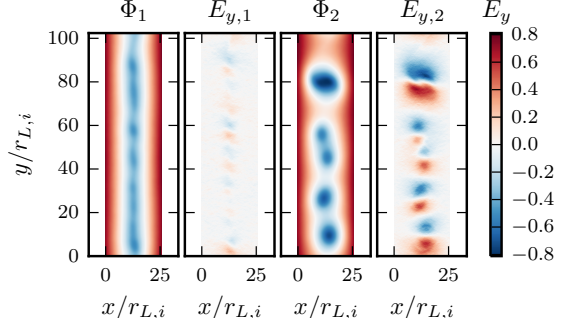


Figure 3: Φ and E_y for the classical KH

Figure 3 shows potential Φ and field component E_y at $\omega_{c,i}t = 18.75$ (linear phase, left) and $\omega_{c,i}t = 43.75$ (nonlinear phase, right). They exhibit vortical structures that are characteristic for the KH instability. Figure 4 shows the growth rates for several spatial modes comparing our results (in black) to the results from [4] and theoretical predictions. The results show good agreement.

Table 1: Plasma parameters for the simulation runs of the plasma-vacuum interface instability

Run	m_i/m_e	$\omega_{c,e}/\omega_{p,e}$	$\omega_{c,i}/\omega_{p,i}$	$r_{L,i}/\lambda_{D,e}$	Box size $L_x \times L_y/r_{L,i}^2$
1	4	2	1	1	50×125
2	16	2	0.5	2	25×62.5
3	100	2	0.2	5	10×25

The Kelvin-Helmholtz instability in a plasma-vacuum boundary layer

Figure 5 illustrates the geometry of the boundary layer. The two-species plasma fills one half of the x - y -plane. Ions (red) move on circular orbits with a larger radius due to their bigger mass. This takes them farther outside the bulk plasma and creates a charge imbalance. An electric field arises, pointing towards the plasma-filled region. In conjunction with the magnetic field, it causes the particles to drift in the negative y -direction.

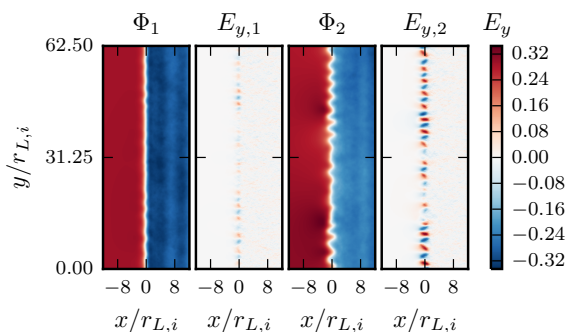


Figure 6: Φ and E_y for the PV KH is higher, resulting in smaller features.

Figure 7 shows growth rates as a function of mode number normalized to the same electron quantities for runs 1–3. In this set of units, the fastest growing mode number as well as the highest growth rates are comparable for all three runs, even though theoretic models for the classical KH instability predict a scaling with the shear layer parameters width (a) and strength (V_0) which vary with mass ratio.

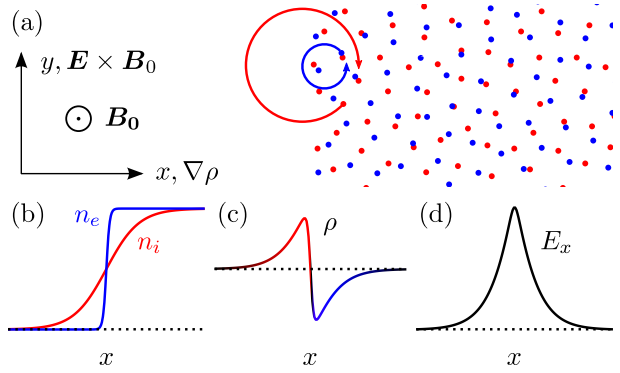


Figure 5: Boundary layer geometry

We perform several simulations of this scenario at different mass ratios. Table 1 summarizes the important parameters.

Figure 6 shows the potential Φ and electric field component E_y at $\omega_{c,i}t = 18.75$ (left) and $\omega_{c,i}t = 31.25$ (right) for run 2. They demonstrate the growth of periodic structures at the PV interface. Compared to the classical KH instability, the dominant spatial mode number

Table 2: Effective shear layer width \tilde{a} and effective velocity shear strength \tilde{V}_0

Run	$a/r_{L,i}$	$V_0/v_{th,i}$	$\tilde{a}/r_{L,i}$	$\tilde{V}_0/v_{th,i}$
1	0.70	0.10	0.36	0.051
2	0.75	0.29	0.18	0.10
3	0.63	0.86	0.072	0.26

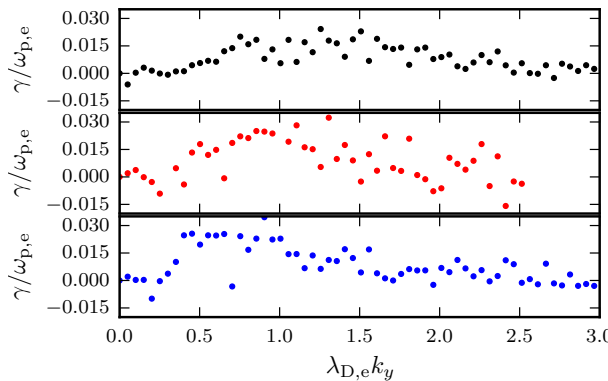


Figure 7: Growth rates for runs 1–3 and the classical model, also found in table 2.

Figure 8 shows the growth rates, this time normalized using the effective parameters. Notably, the three results show a certain similarity also to one another, especially a suppression of low wave number unstable modes. Comparing the actual and effective parameters in table 2, the KH instability in the PV scenario can be said to be similar to a classical instability with a reduced shear layer width and shear strength.

Conclusions

In this work, we have compared our novel method to both theory and traditional PIC methods using simulations of well-understood plasma phenomena. We have also presented a new scenario for a KH type instability in plasmas and studied its growth rates.

Acknowledgments

Funding for this work was provided in part by the Helmholtz International Research Group 0048. Computing time on the systems at Jülich Supercomputing Centre was provided by the JARA HPC project JZAM04. The work of RDS is supported by the Natural Sciences and Engineering Research Council (NSERC) of Canada.

References

- [1] M. Winkel et al., Computer Physics Communications **183**, 880 (2012)
- [2] B. Steinbusch et al., Advances in parallel computing **27**, 439 (2016)
- [3] B. Steinbusch, P. Gibbon and R.D. Sydora, Physics of Plasmas **23**, 052119 (2016)
- [4] D. Cai, L.R.O. Storey and T. Itoh, Physics of Fluids B **5**, 3507 (1993)
- [5] I.B. Bernstein, Physical Review **109**, 10 (1958)

We determine a and V_0 from an analysis of all particle trajectories, see table 2. However, a normalization using these actual parameters does not lead to self-similarity between the three results, nor does it make the results compatible with the model for the classical KH instability. We determine a set of effective parameters \tilde{a} and \tilde{V}_0 by performing a least squares fit between the growth rate spectra

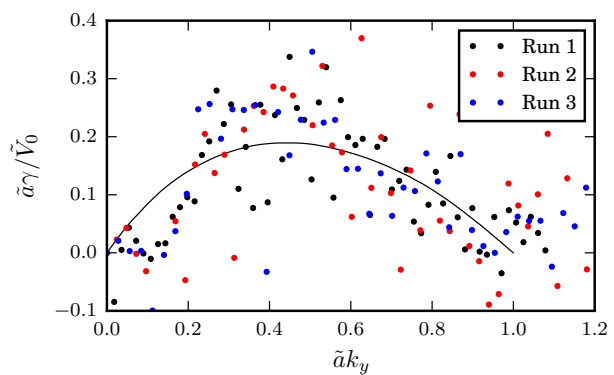


Figure 8: Fitted growth rates